HHS Public Access

Author manuscript

J Immunol. Author manuscript; available in PMC 2018 February 16.

Published in final edited form as:

J Immunol. 2017 February 15; 198(4): 1706–1717. doi:10.4049/jimmunol.1601310.

Subclinical HSV-1 infections provide site-specific resistance to an unrelated pathogen

Alexander M. Rowe[#,*], **Hongming Yun**[#], **Benjamin R. Treat**[#], **Paul R. Kinchington**[#,‡], and **Robert L. Hendricks**[#,‡,¶]

[#] Department of Ophthalmology, University of Pittsburgh School of Medicine

[‡] Department of Microbiology and Molecular Genetics, University of Pittsburgh School of Medicine

[¶] Department of Immunology, University of Pittsburgh School of Medicine

Abstract

Herpes Simplex Virus-1 (HSV-1) infections of the cornea range in severity from minor transient discomfort to the blinding disease Herpes Stromal Keratitis (HSK), yet most patients experience a single episode of epithelial keratitis followed by reestablishment of a clear cornea. We asked if a single transient episode of HSV-1 epithelial keratitis causes long-term changes in the corneal microenvironment that influence immune responses to subsequent corneal infection or trauma. We showed that C57BL/6 mouse corneas infected with HSV-1 KOS, which induces transient herpes epithelial keratitis without HSK sequelae, possessed a significant leukocytic infiltrate comprised primarily of $CD4^+$ T cells and macrophages along with elevated chemokines and cytokines that persisted without loss of corneal clarity (subclinical inflammation). Chemokine and cytokine expression was $CD4^+$T cell-dependent, in that their production was significantly reduced by systemic $CD4^+$T cell depletion starting before infection, although short-term (3 day) local $CD4^+$ T cell depletion after infection did not influence chemokine levels in cornea. Corneas with subclinical inflammation developed significantly greater trauma-induced inflammation when they were recipients of syngeneic corneal transplants, but also exhibited significantly increased resistance to infections by unrelated pathogens such as pseudorabies virus (PRV). The resistance to PRV was $CD4^+$ T cell-dependent, since it was eliminated by local $CD4^+$T cell-depletion from the cornea. We conclude that transient HSV-1 corneal infections cause long-term alterations of the corneal microenvironment that provide CD4-dependent innate resistance to subsequent infections by antigenically unrelated pathogens.

Introduction

Viral infections of skin or mucosa generally leave a resident memory cell population behind at the site of infection [1]. Herpes simplex virus type 1 (HSV-1) is a common cause of corneal infectious keratitis in which infections of the cornea leave behind a pathogenic immune infiltrate that reduces clarity [2]. Ocular HSV-1 pathologies of the cornea can be divided into two general types. The less common, but far more visually debilitating, of the

[*] **Address correspondence to**: Alexander M. Rowe, University of Pittsburgh, Eye and Ear Institute, 203 Lothrop Street, Pittsburgh, PA 15213.

two are lesions of the corneal stroma, termed herpes stromal keratitis (HSK). These lesions are immunologically mediated, can occur in the absence of detectable replicating virus, and can cause permanent visual impairment due to scarring [3]. In humans, HSK is mediated by a pathogenic, possibly HSV-1 specific T cell population [4, 5]. More common than HSK is epithelial keratitis. Epithelial keratitis involves pathognomonic dendritic or geographic-shaped lesions in the corneal epithelium, where virus replication and destruction of corneal epithelial cells occurs [6]. These lesions generally resolve without permanent visual impairment [7]. The long-term subclinical effects of epithelial keratitis on the immune responses of the cornea need to be investigated, because epithelial disease is often the first step towards blinding HSK.

In the murine model, primary HSV-1 infection of corneas results in epithelial lesions that resemble the dendritic or geographic herpes epithelial keratitis seen in humans [2]. In mice, as in humans, epithelial lesions do not necessarily progress to HSK [7, 8]. Factors contributing to the different pathological outcomes of HSV-1 infections include the initial infectious dose and genotype of both the host and the virus. Indeed, murine HSV infections can be manipulated experimentally to favor certain disease states by varying these factors. For instance, corneal infections of BALB/c mice with the KOS strain of HSV-1 results in sequential development of epithelial lesions followed by HSK, whereas similar infections of C57BL/6 mice cause epithelial lesions without progression to HSK [9, 10]. Following resolution of HSV-1 KOS-induced epithelial keratitis, the corneas of the majority of C57BL/6 mice lack any visually detectable signs of infection or inflammation. The immunopathology of HSK is well-defined [9-12], but little is known about what, if any, long term effects the immune response to acute epithelial keratitis has on the corneal microenvironment and its susceptibility to subsequent infections.

It is increasingly apparent that an individual's health is not maintained simply by the absence of infection, but by good immunological management of infections. Intracellular pathogens induce site-specific immunity in non-lymphoid tissue [13, 14]. We hypothesized that the local memory response to acute herpes epithelial keratitis may be beneficial to the host in modulating subsequent infections or trauma. This hypothesis was intuited because of the co-evolution of HSV-1 and humanity [15], the ubiquitous nature of HSV-1 infections, and the lack of effective herd immunity [16, 17]. Our hypothesis does have some precedent, as chronic gamma herpes virus infections induce a systemic inflammation that provides intrinsic resistance to subsequent novel immunological challenges [18], and acute viral infections induce tissue-resident memory (Trm) $CD8^+$ T cells that, when activated, provide intrinsic resistance to unrelated pathogens [19]. In addition, alpha herpes infections such as HSV-1 and 2 are known to leave an immunological foot print at the site of infection [14, 20, 21].

We demonstrate that mouse corneas with resolved HSV-1 epithelial lesions that do not progress to HSK, nonetheless maintain a prolonged and significant subclinical immunological response. Unlike other viral infections in the skin or lungs that leave a predominantly $CD8^+$-dominated Trm infiltrate [13, 14], the resolved corneal infections leaves a $CD4^+$ T cell-dominated infiltrate, elevated levels of cytokine and chemokine expression but almost no $CD8^+$ T cells. We show that the effects of the subclinical

inflammation on the health of the cornea are, at best, a double-edged sword. The subclinical infiltrate of the cornea renders it more susceptible to subsequent trauma-induced inflammation, but at the same time, more resistant to subsequent infection with an unrelated pathogen.

Methods

Mice

Female wild type C57BL/6 mice were purchased from Jackson Laboratories (Bar Harbor, Maine) and housed in the University of Pittsburgh vivarium. Mice were allowed at least one week of acclamation prior to use in experiments. The use of animals was in accordance with the Association for Research in Vision and Ophthalmology Statement for the Use of Animals in Ophthalmic and Vision Research, and all procedures were approved by the University of Pittsburgh Institutional Animal Care and Use Committee.

Viruses and Infections

The HSV-1 strains KOS [22] (a generous gift from Dr. Donald Coen) and HSV-1 RE [23] (generous gift from Dr. Robert Lausch) were maintained as low passage stocks in our laboratory. Strain identity was confirmed by sequencing the viral DNA at key sites, including a marker diagnostic for KOS [24] and the US9 regions (see GenBank: KF498959.1). Pseudorabies virus (PRV) used in this study were generated using a Becker-strain bacterial artificial chromosome (BAC) (kind gift from Lynn Enquist, Princeton University NH). A thymidine kinase knockout virus was developed by insertion of a kanamycin-resistance cassette and monomeric red fluorescent protein (mRed), amplified using the following primers: Forward, 5'gcggcaacctggtggtggcctcgctggacccggacgagcacatggcctcctccgaggacgtcat3';Reverse, 5’tcaggtagcgcgacgtgttgaccagcatggcgtagacgttttattaggcgccggtggagtggcgg3’ and the plasmid pMred- kan in. The kanamycin-resistance cassette was subsequently resolved using red-mediated recombination, and virus was then obtained from BAC transfected Vero cells. PRV was subsequently propagated to high titer in PK15 (porcine kidney 15) epithelial cells and purified.

HSV-1 infections were carried out using wild-type female C57BL/6 mice between 6 and 12 weeks of age. Briefly, the mice were anesthetized by intraperitoneal injection of a mixture of ketamine and xylazine (Henry Schein Animal Health, Dublin Ohio) at doses of 100 and 11 mgs per kilogram of body weight, respectively. Subsequently, the corneas of anesthetized mice were scarified using a 30-gauge needle. The scratches on the corneal epithelium were deep enough to reach but not penetrate the basement membrane. Three μl of PBS (mock infection) or PBS containing 1×10^5 plaque forming units (pfu) of HSV-1 strains KOS or RE or Pseudorabies virus lacking thymidine kinase (PRV-TKO) were then applied directly to the scarified corneas. The effects of anesthesia were then reversed by injecting mice with 10 μg of atipamezole hydrochloride (Henry Schein Animal Health, Dublin OH).

Corneal Transplantation

Syngeneic (C57BL/6) orthotopic corneal transplantations were performed on age matched groups of mice. HSV-1 KOS-infected recipient corneas were examined prior to transplantation and rare mice with neovascularization and/or opacity scores of 1 or greater in any area of the cornea (see scoring below) were excluded from the study. Donor corneal buttons (2 mm diameter) were excised from non-infected C57BL/6 mice and transplanted onto the recipient corneal graft bed. The recipient mice were anesthetized with a mixture of ketamine and xylazine (Henry Schein Animal Health, Dublin Ohio) as described for corneal infections above. The cornea graft was secured with eight interrupted 11-0 nylon sutures (Sharpoint, Nylon black monofilament, 5”/13cm, 0.1 metric, 11-0, Surgical Specialties Corporation, Reading, PA, 19606, USA). Sutures were removed from the graft at 7 days post-transplant.

Assessment of Viral Replication in the Cornea

Viral replication was assessed by eye swab at various days post-infection (dpi). A sterile tube was filled with 500 μl of either sterile HBSS or PBS. A sterile surgical spear (Catalog # 008680, Beaver Visitec, Sydney, Australia) was soaked in the sterile buffer and then the surface of the cornea was brushed with the swab twenty times. The swab was then returned to the tube and stored at −80°C. The number of viral pfu per swab was determined via plaque assay. African green monkey kidney cells (Vero cells:-ATCC CLL-81) were grown to confluence in a sterile 48 well tissue culture plate (Becton Dickinson, Franklin Lakes, NJ) were used to enumerate the number of pfu per swab. All excess media was removed from the cell layer. The fluid contents of the swab tubes was diluted in sterile in PBS or HBSS and applied to the cell layer in a volume of 100 μl. Each swab was plated in triplicate. The plates were then incubated for 1 hour before a methylcellulose containing media was laid over the cells to prevent viral spread. The infected plates were incubated for 48 hrs. The media was removed, the cells were fixed with 10% Buffered Formalin Phosphate (Catalog Number SF100-4, Fisher Scientific, Fair Lawn NJ) and then stained with 1% Gentian Violet (Ricca Chemical Company, Arlington TX). The plaques per well were counted and the number of plaques forming units per swab were calculated. The same protocol was used for assessing PRV and HSV-1 replication in the cornea.

Assessment of Ocular Pathology

Epithelial lesions, indicating viral replication, were assessed two days after infection with HSV-1 or PRV using Fluorescein sodium (Akorn Inc, Lake Forest IL) in sterile PBS at 0.1 mg/ml. Fluorescein drops were applied to the eyes and the lesion visualized under a blue light using an Olympus SZX16 Stereomicroscope (Olympus America Inc, Center Valley, PA). Lesions were scored on five point scale; 0=no visible fluorescein uptake in the cornea, 1=punctate lesions in the cornea, 2=dendritic lesions in the cornea, 3=geographic lesions and dendritic lesions taking up less than 25% of the corneal area, 4= dendritic and geographic lesion taking up more than 25% of the corneal surface.

Corneal pathology was scored for three symptoms: neo-vascularization, corneal opacity and corneal sensation. Corneal neo-vascularization was examined using a stereoscope (Model Z30 L, Cambridge Instruments, Sommerville, MA) and was scored in each quadrant from 1

to 4, to give a total measurement on a 16 point scale: 0 = no vessels visible, 1= vessels extending into the corneal bed, 2 = vessels extending 25-50% towards the corneal center, 3 = vessels extending more than 50% of the way towards the corneal center but not reaching the center of the cornea or 4 = vessels extending to the central cornea. Opacity was also scored by visualization of each quadrant, scored as follows: 0 = clear; 0.5 = small isolated imperfections or regions of translucence; 1 = minimal translucence or haziness extending over region but allowing visualization of the iris; 1.5 = translucence or haziness extending over the quadrant with small punctate regions of opacity; 2 = cloudiness and regional opacity allowing only heavily distorted visualization of the iris; 2.5 = opacity extending of over the entire quadrant with punctate regional translucence allowing very limited and strongly obscured visualization of the iris; 3 = complete stromal opacity with no visualization of the iris structures; 3.5 = complete stromal opacity associated with associated pathology such a granuloma or ulcer; 4 = perforation of the cornea. Hypoesthesia was measured regionally on a five point scale, with a score of five being complete sensitivity and score of zero being a cornea completely insensitive to topical physical stimuli. Using a sterile plastic probe, the cornea was touched in four peripheral regions and central region. If the mouse responds to the touch of the probe that region of the cornea is scored as positive.

Scoring of corneal grafts was done in much the same manner, with minor variations that took into consideration the specific nature of the graft. For judging vascularization following grafting, the eye was visually divided in 4 quadrants and each quadrant was scored on a 4 point scale: 0 = no vessels visible; 1= vessels extend into the corneal bed; 2 = vessels extending up to graft-interface; 3 = vessels extending into the graft but not reaching the center of the graft; or 4 = vessels extending to the central graft. Assessment of opacity was limited to the graft only; scores reflect opacity in the graft and not the supporting corneal bed. Graft scoring used a 16 point system as described above. Images of corneas in live mice were acquired using an Olympus SZX16 Stereomicroscope and an Olympus DP80 digital camera (Olympus America Inc, Center Valley, PA).

Assessment of Corneal mRNA

Total RNA from corneas was obtained using RNeasy kit, as per manufacturer's instructions (Qiagen, Germantown MD). The relative levels of specific mRNAs were assessed using a custom designed NanoString^{R} array (NanoString Technologies, Seattle, WA) or by real time PCR. NanoString^{R} analysis was performed by applying purified RNA directly to the NanoString^{R} chip, as per manufacturer's instructions. Relative gene expression was normalized to a panel of housekeeping genes (**see Table 1**). Preparation of cDNA synthesis was performed on 2 μg of total RNA prepared from corneal homogenates, using a high capacity cDNA Reverse Transcriptase kit (Applied Biosystems, US). Real-time PCR primers were derived and quantified using a FAM-labeled MGB Taqman^{R} probe for each gene (Applied Biosystems, US). The probes recognized CXCL10 (Mm_00445255_ml), CXCL9 (Mm_0043946_ml), CCL5 (Mm_01302427_ml) and Histone H1 (Mm_00469312_ml).

Assessment of viral copy number and viral mRNA in the trigeminal ganglion (TG)

Viral DNA copy number was assessed by using a real time PCR protocol employing a labelled probe (5’-(FAM)TCCGGACCACTTTTC(NFQ)-3’),that recognizes the gene for

glycoprotein H (gH). The reaction was carried out using TaqMan^R Universal PCR Master Mix. Because HSV-1 contains a single copy of gH, we compared the Ct values to that of a plasmid standard and then used a liner regression to calculate copy number. Briefly, the TGs were placed into a DNA-preserving tissue digestion buffer purchased from Qiagen (Qiagen, Germantown MD). The tissue was digested with proteinase K and the DNA was isolated using Qiagen DNeasy kit, as per manufacturer's instructions. Mathematical and statistical analysis was performed using Applied Biosystems StepOne software (Thermo Fisher Scientific Waltham, MA) and GraphPad Prism Software (GraphPad Software, Inc, La Jolla, CA). Latency-associated transcript (LAT) was quantified using a TaqMan^R RT PCR assay as described above and the forward LAT forward primer 5′GCATAGAGAGCCAGGCACAAAA3′; and the reverse primer 5′ACGTACTCCAAGAAGGCATGTG3′. These and the probe were previously described and validated previously [25].

In Vivo Depletions

For systemic CD4 depletions, mice were injected intraperitoneally with 100 μg of anti-CD4 clone GK1.5 (Bioxcell, Lebanon, NH) starting two days prior to infection. Injections with 100 μg of anti-CD4 were repeated at 1 day and 4 days post-infection, then every six days until the time of sacrifice or PRV infection. Local CD4 depletions were carried out via subconjuctival injections using a Hamilton syringe (Hamilton Company, Reno, NV). Local CD4 depletions (30 μg of clone GK1.5 in a volume of 20-40 μl of sterile PBS) were given three days before PRV infection. Depletion of macrophages was achieved using a mixture of clordonate liposomes (Molecular Cell Biology and Immunology, Amsterdam, Netherlands) and anti-Ly6C antibody (Monts-1 clone, Bioxcell, Lebanon, NH). The 20 μl of liposomes were diluted 1 to 1 with sterile PBS mixture containing 70μg anti-Ly6C for total volume of 40μl. The mixture was administered subconjunctivally via a single injection using a Hamilton syringe. We observed no leakage of this volume, and the efficacy of the depletions was confirmed by flow cytometry (Fig 6).

Ex Vivo Stimulations

Spleens from naïve female C57BL/6 mice were harvested, triturated into a single cell suspension and depleted of $CD4^+$ T cells using an EASY-SEP PE selection kit and anti-TCR beta (clone H57-597) and anti-CD4 (clone RM4-5), both conjugated to phycoerythrin (PE). The depleted splenocytes were then infected with HSV-1 KOS or PRV at an MOI of 1 and incubated for eight hours at 37°C in RPMI media supplemented with 10% FBS (Atlanta Biologicals). Spleens from female C57BL/6 mice infected with PRV Becker or HSV-1 KOS (as described above) were harvested at 9 or 10 days post-infection, elutriated into single cell suspension and the cells counted. The $CD4^+$ T cell were enriched using an EASY-Sep mouse CD4 T-cell enrichment kit. T cell enrichment was assessed by flow cytometry, cells were stained with PE-Cy7 conjugated anti-CD4 (RM4-5), FITC-conjugated anti-CD8α (53-6.7), APC-Cy7-conjugated anti-CD11b (M1/70), and anti-CD44 conjugated to V450 (clone IM7). All antibodies were purchased from BD Biosciences, San Diego CA. $CD4^+$ T cell purity ranged from to 85-93%. The enriched $CD4^+$ T cells were placed into culture with the infected or uninfected splenocytes for 5 hours in the presence of Brefeldin A. The cells were then treated with anti-mouse CD16/CD32 (Fcγ III/II receptor; 2.4G2; BD PharMingen, San

Diego, CA) to prevent nonspecific antibody binding and then stained with Vital dye (LIVE/DEAD fixable Aqua, Molecular Probes, Eugene OR) and antibodies for the surface markers list above for 30 min at room temperature in PBS. After staining, the cells were fixed with BD Cytofix/Cytoperm for 20 minutes at 4°C (cat# 554722, BD Bioscience, San Diego, CA) and then permeablized with BD Perm/Wash (cat# 554723, BD Bioscience, San Diego, CA). The cells were stained intracellularly with Rat anti-mouse IFN-γ conjugated to APC (cat#554413, BD Bioscience, San Diego CA). The cells were analyzed by flow cytometry using a live-cell gate.

Characterization of T cells in the TG and DLN

Female C57BL/6 mice with or without HSV-1 KOS infections were infected via the cornea with 1×10^5 pfu of PRV. At 9 dpi the mice received an i.p. injection with 100 μg of BrdU (Sigma, St. Louis, Missouri). Four hours post-injection the mice were anesthetized and exsanguinated. The TGs were harvested and incubated for 1 hour in 0.2 units of Liberase TM (catalog # 05 401 127 001, Roche). The TGs were then washed and passed through 40 μM nylon mesh filter. DLN cell were mechanically worked into single suspensions and passed through a 40 μM nylon mesh filter. Cells were treated with anti-mouse CD16/CD32 (Fcγ III/II receptor; 2.4G2; BD PharMingen, San Diego, CA) to prevent nonspecific antibody binding and then stained for various leukocyte surface markers for 30 min at 4°C. BrdU staining was carried out using a BrdU staining and fixation kit (BD PharMingen, San Diego, CA) as per manufacturer's instructions, with the supplementation of DNAse I purchased from Sigma (St. Louis, Missouri). Staining was assessed on a flow cytometer (FACSAria, BD Bioscience), and analyses was carried out using FlowJo software (Tree Star Inc., Ashland, OR). The lymphocytes from the DLNs were gated on size prior to analysis of subpopulations. The cells in the TG were gated on CD45 expression prior to analysis of subpopulations.

Characterization of Corneal Immune Infiltrates

The corneas were incubated for 1 hour at 37°C in 0.4 units of Liberase TM (catalog # 05 401 127 001, Roche) in a volume of 100 μl of buffer, then triturated with a 200 μl pipette tip and passed through a 40 μM nylon mesh filter. Corneal cells were washed and stained for analysis via flow cytometry. Various panels of antibodies were used dependent on the experiment. Corneal cells were treated with anti-mouse CD16/CD32 (Fcγ III/II receptor; 2.4G2; BD PharMingen, San Diego, CA) to prevent nonspecific antibody binding and then stained for various leukocyte surface markers for 30 min at 4°C. The following antibodies were purchased from BD Pharmingen: phycoerythrin (PE)-conjugated anti-GR-1 (RB6-8C5), fluorescein isothiocyanate (FITC)-conjugated, PE-Cy7 conjugate or AlexaFluor647 conjugated anti-CD4 (RM4-5), peridinin chlorophyll protein (PerCP)-conjugated anti-CD45 (30-F11), allophycocyanin (APC) or FITC-conjugated anti-CD8α (53-6.7), and eFluor450-conjugated anti-CD11b (M1/70). Anti-F4/80 (clone BMB) conjugated to PE-Cy7 was purchased from eBioscience (San Diego, CA). Anti-TCR beta (clone H57-597) conjugated to AlexaFluor647 was purchased from BioLegend (San Diego, CA). For analysis of surface marker only, cells were fixed in 1% paraformaldehyde (PFA; Electron Microscopy Sciences, Fort Washington, PA), staining was assessed on a flow cytometer (FACSAria, BD Bioscience), and analyses was carried out using FlowJo software

(Tree Star Inc., Ashland, OR). For transcription factor staining cells were fixed following a surface staining protocol using a BD Pharmingen Transcription Factor Buffer Set (Catalog # 562725, BD Pharmingen, San Diego, CA). T-bet was stained with BV421 conjugate to O4-46 clone and FOXP3 was stained using PE conjugate MF23 clone also obtained from BD Pharmingen.

Immunohistochemistry

As described previously, mouse corneas were dissected, fixed and then processed for whole mount immunohistochemistry staining. Briefly, nerve fibers were stained with primary antibodies that included: rabbit polyclonal anti-Beta III tubulin (cat #ab18207), chicken polyclonal anti-tyrosine hydroxylase (TH, cat #76442), all from Abcam, Cambridge, MA; or mouse monoclonal antibody to calcitonin gene related peptide (CGRP ab81887 LOT GR158523-12). Secondary antibodies included: Alexa Fluor 488 goat anti-rabbit IgG (H+L) (cat #GR233725-3, Abcam, Cambridge, MA, USA); Alexa Fluor 546 goat anti-chicken IgG(H+L) (cat #1618409, Life Technologies, Grand Island, NY, USA); Alexa Fluor 647 goat anti-mouse IgG1 (cat# A-11040) from Invitrogen The corneas were also stained with 4'-6-diamidino-2-phenylindole (DAPI Sigma, St. Louis, MO).

Results

A model of transient HSV-1 epithelial keratitis

We examined the course of HSV-1 infections in C57BL/6 mice infected with the RE strain, which causes HSK, and the KOS strain, which does not. Both virus strains have a disrupted US9 gene (P.R. Kinchington, unpublished data) and the two strains cause similar corneal epithelial lesions (Fig 1 A&B) and HSK in BALB/c mice [10]. Moreover, side by side infections of C57BL/6 mice with RE and KOS strains of HSV-1 revealed similar levels of viral replication in the eye (Fig. 1A-C). Replicating virus was not detectable in the tear film beyond 6 dpi (data not shown). The viruses established similar latency in trigeminal ganglia, as measured by the number of viral genome copies and expression of the Latency Association Transcript (Fig. 1G&H). However, the RE strain induced clinically apparent HSK in the majority of the mice, whereas the KOS strain did not (Fig. 1D&E). The KOS infection induced a partial reduction in corneal sensitivity (as assessed by blink reflex) (Fig. 1F), in contrast to the rapid and complete loss of sensitivity in RE-infected corneas (Fig. 1F). Consistent with our previous work, only the complete loss of sensitivity observed in RE infected corneas was associated with development of severe corneal opacity (Fig. 1E-F). Because our goal is to characterize the long-term consequences of a subclinical HSV-1 induced inflammation, we subsequently focused on KOS-infected mice that developed transient epithelial keratitis without progression to HSK.

“Subclinical Inflammation” persists in KOS HSV-1 infected

The leukocytic infiltrate was assessed after KOS HSV-1 clearance (9 and 34 dpi) in C57BL/6 corneas that lacked overt pathology (Fig. 2A&B). The leukocytic infiltrate in non-infected corneas was negligible (Fig. 2C). At both 9 and 34 dpi the infiltrate was dominated by $CD4^+$ T cells and $CD11b^+$ myeloid cells, but while the number of $CD4^+$ T cell did not significantly change between the time points (Fig. 1D), the ratio of $CD4^+$ cells to $CD11b^+$

cells did increase (Fig. 2A&B, and data not shown). The $CD11b^+$ cells present at 34 dpi were predominantly $F4/80^+$ macrophages and lacked a $F4/80^-C11b^{hi}Gr\text{-}1^{hi}$ neutrophil population (staining not shown). At 9 dpi, the $CD4^+$ population expressed more T-bet^+, both as a percentage of the population and in terms of MFI than was expressed by corneal $CD4^+$ T cells at 34 dpi (Fig. 2E-H). $FoxP3^+$ Tregs comprised about 10% of the $CD4^+$ T cell infiltrate at both 9 and 34 dpi (Fig. 2E&F).

Consistent with the changes in T-bet expression [26], we observed that the levels of the inflammatory cytokine IFN-γ were not elevated above that found in naïve mice past 15 dpi (Fig. 2I, one-way ANOVA comparing days post-infection followed by Dunn's post-test). However, chemokines such as CCL5, CCL2, CCL22 CXCL10, and CXCL9 were continually expressed at significantly higher levels in previously HSV-1 infected corneas (Fig 2I). Direct analysis of expression at 34 dpi by both Nanostring^R and RT-PCR found that the above chemokines were expressed at levels significantly greater than naïve mice but inflammatory cytokines such IL-17 and IFNγ were not (Fig 2I and data not shown). Corneal HSV-1 infections are known to change corneal nerve phenotype in addition to function [9, 10, 12]. Thus, the corneas were also examined for qualitative changes in the nerves innervating KOS and RE infected corneas (Supplemental Figure 1). As previously reported [10], non-infected corneas contain only sensory nerves ($CGRP^+$ neurons) and that corneas with severe HSK contain only sympathetic (TH^+) but not sensory (CGRP+) nerves. Interestingly, KOS infected corneas with subclinical inflammation possessed both sensory and sympathetic neurons (Supplemental Fig 1C).

KOS HSV-1 infection increases corneal inflammation following surgical insult

We tested the hypothesis that the subclinical inflammation in KOS HSV-1 infected C57BL/6 mouse corneas would increase corneal sensitivity to clinical inflammation following surgical trauma. To test this, orthotopic syngeneic C57BL/6 corneal grafts were placed on normal corneal beds or corneal beds with subclinical inflammation 28-34 days after KOS HSV-1 infection. All grafts received a temporary tarsorrhaphy to protect the cornea until the sutures were removed from the graft 7 days after transplant. Examination of the grafts immediately after removal of the tarsorrhaphy revealed significantly more inflammation in HSV-1-infected corneas compared to non-infected corneas (Fig. 3A&B). Graft opacity was then monitored through 40 days after transplant. The level of opacity was significantly higher in grafts placed on KOS HSV-1-infected corneal beds with subclinical inflammation, when compared to those placed on non-infected beds (Fig. 3C&D), although neither achieved a level of opacity that would be considered rejection in most studies [27-29].

Subclinical inflammation in KOS HSV-1 infected corneas provides local intrinsic resistance to unrelated viral infections

HSV-1 KOS infected corneas with subclinical inflammation, the contralateral non-infected cornea, or corneas of non-infected mice were infected with 1×10^5 pfu of PRV. Eyes were swabbed at 1 and 4 days post challenge and shed virus was quantified in a viral plaque assay. One day after PRV infection, PRV titers in swabs of previously HSV-1 infected but clinically uninflamed corneas were significantly lower than titers in either the contralateral non-infected corneas of the same mice, or in corneas of previously non-infected mice (Fig. 4A).

Fluorescein staining revealed significantly (p=0.003) smaller PRV-induced corneal epithelial lesions in previously HSV-1 infected corneas as compared to previously non-infected corneas (Supplemental Fig 1 D). PRV titers in non-infected corneas contralateral to HSV-1-infected corneas were not significantly different from those in previously non-infected mice (Fig 4A). Thus, protection from PRV is not systemic, but rather restricted to the microenvironment of the previously HSV-1 infected, but clinically uninflamed cornea. Shedding of PRV was undetectable in all treatment groups at 4 and 6 dpi (data not shown). Prior to PRV-1 challenge, the $CD45^+$ corneal infiltrate in HSV-1 infected corneas with subclinical inflammation was dominated by $CD4^+$ T cells (Fig. 1B), but at 24 hrs after PRV infection, the immune infiltrate was dominated by $CD11b^+$ cells (Fig. 4B&C). The corneal $CD11b^+$ population 24 hrs post-PRV infected was a roughly 50/50 split of neutrophils and $CD11b^+$ macrophages (Fig. 4C). The mean number of $CD45^+$ cells was consistently greater in previously HSV-1 infected corneas compared to the non-HSV-1 infected corneas (Fig. 4B&C). This increase was due in part to the presence of a $CD4^+$ T cell population in HSV-1 infected corneas that was absent from non-infected corneas both prior to or after PRV challenge (Fig. 4B&C). The size of the overall $CD11b^+$ population and the neutrophil population tended to be higher in the HSV-1 infected mice, although the difference was not statistically significant in the majority of experiments (Fig. 4C). Mice infected with the attenuated PRV virus developed ocular pathology characterized by corneal hypoesthesia, opacity and vascularization of the cornea. Interestingly, the severity of that pathology was significantly reduced in mouse corneas that were previously infected with HSV-1 (Supplemental Fig. 1 D-F).

A $CD4^+$T cell response is necessary for intrinsic resistance to unrelated viral pathogens

The fact that $CD4^+$ T cells are the dominant immune cell population in the previously HSV-1 KOS infected corneas with subclinical inflammation, suggested their possible involvement in enhanced PRV clearance. We initially tested whether $CD4^+$ T cells are required to maintain the elevated chemokine levels in HSV-1 infected corneas with subclinical inflammation. $CD4^+$ T cells were depleted systemically by i.p. injections of anti-CD4 antibody, starting 2 days prior to HSV-1 infection and continuing at weekly intervals through 34 dpi. Flow cytometry demonstrated that there were no $CD4^+$ T cells in the corneas of depleted mice at 34 days following an HSV-1 infection (data not shown). We found that systemic $CD4^+$ T cell-depletion dramatically reduced mRNA levels of multiple chemokines in infected corneas that lacked clinically observable inflammation (Fig. 5A). Moreover, $CD4^+$ T cell-depletion eliminated the enhanced PRV clearance in previously HSV-1 infected corneas (Fig. 5B).

Since $CD4^+$ T cell-depletion reduced chemokine levels in HSV-1 infected corneas prior to PRV infection, we proposed that the reduced PRV clearance would be associated with a reduced immune infiltrate in HSV-1 infected corneas of $CD4^+$ T cell-depleted mice. The CD4 depleted mice did have a $CD8^+$ T cell infiltrate in the cornea that previously uninfected mice and HSV-1 infected CD4 replete mice did not (Fig. 5 C). The infiltration of $CD8^+$ T cells into the corneas of CD4 depleted mice infected with HSV-1 has been previously described [30]. Surprisingly, the HSV-1 infected corneas of $CD4^+$ T cell-depleted mice

showed a higher $CD45^+$ infiltrate 24 hrs after PRV infection compared to HSV-1 infected corneas that were not $CD4^+$ T cell-depleted (Fig. 5D).

Since $CD4^+$ T cells were required for enhanced PRV clearance in HSV-1 infected corneas, we considered that the enhanced clearance might reflect antigen cross reactivity between PRV-specific and HSV-1-specific $CD4^+$ T cells. However, ex vivo stimulation of T cells from HSV-1 and PRV infected mice did not reveal cross reactivity. Thus, $CD4^+$ T cells from HSV-1 infected mice responded to HSV-1 infected but not PRV infected APCs, whereas T cells from PRV infected mice responded to PRV infected but not HSV-1 infected APCs (Fig. 5E).

Tissue resident macrophages are not required for HSV-1-induced resistance to PRV

In addition to $CD4^+$ T cells, the next most abundant immune population in HSV-1 KOS infected corneas is $CD11b^+F4/80^+Gr\text{-}1^{neg\text{-}int}$ macrophages (Fig 2, and data not shown). We considered that $CD4^+$ T cells might mediate nonspecific clearance of PRV indirectly by priming a memory macrophage response. To test whether the tissue resident macrophages are required for enhanced PRV clearance, we depleted macrophages from HSV-1 infected corneas prior to PRV infection. Mice with HSV-1-induced subclinical corneal inflammation received subconjuctival clodronate liposomes and anti-Ly6C antibody (Monts-1 clone), or PBS-liposomes alone 7 days before PRV infection, and corneal infiltrates were assessed 24 hrs after PRV infection. The clodronate liposome treatment effectively depleted macrophages from HSV-1 infected corneas prior to PRV infection (Fig. 6A). However, depleting macrophages that were resident in the HSV-1 infected corneas prior to PRV infection did not influence the overall $CD45^+$ population or the $CD11b^+$ population in corneas 24 hrs after PRV infection (Fig. 6B), and did not influence PRV clearance from the cornea (Fig. 6C).

Local depletion of $CD4^+$ cells inhibits viral clearance without decreasing chemokine expression

In studies described above, systemic $CD4^+$ T cell-depletion reduced chemokine levels and eliminated enhanced PRV clearance in HSV-1 infected corneas with subclinical inflammation (Fig 4). It was not clear if $CD4^+$ T cells were required locally in the cornea or mediated these effects systemically. To address this, C57BL/6 mice received KOS HSV-1 corneal infections, and at 28-34 dpi HSV-1 infected mice and non-infected control mice were locally depleted of $CD4^+$ T cells by subconjunctival injection of anti-CD4 mAb or mock depleted. Three days later the corneas were excised and dispersed cells were shown to lack detectable $CD4^+$ or $CD8^+$ T cells by flow cytometry (Fig. 7A&B).

RNA was extracted from HSV-1 infected corneas three days after local $CD4^+$ T cell-depletion or mock depletion and analyzed for CXCL9 and CCL5 transcripts by qRT-PCR. The levels of CXCL9 and CCL5 mRNA were not reduced in HSV-1 infected corneas 3 days after local $CD4^+$ T cell-depletion (Fig. 7C). PRV corneal infections were performed 3 days after $CD4^+$ T cell-depletion or mock depletion of HSV-1 infected or non-infected corneas. Twenty-four hrs after PRV infection, dispersed corneal cells were analyzed by flow cytometry (Fig. 7D-F). The $CD4^+$ T cell-depleted HSV-1 infected corneas exhibited

comparable CD11b^{high}, Gr-1^{high} neutrophil and CD11b^{high}, Gr-1^{low} macrophage populations to the mock depleted corneas (Fig. 7D-F), but lacked detectable CD4$^+$ or CD8$^+$ T cells (Fig. 7E). Local depletion of CD4$^+$ T cells did eliminate the enhanced clearance of PRV from HSV-1 infected corneas (Fig. 7G).

Discussion

The cornea is unique among mammalian tissue in that it is continually exposed to the environment, is not vascularized, and its function requires transparency. Indeed, the cornea has developed a degree of immune privilege in an apparent attempt to prevent loss of vision due to vascularization and opacity [31]. However, certain types of infectious and non-infectious trauma can overcome the corneal immune privilege leading to a clinically inflamed cornea. An interesting example is HSV-1, wherein the clinical outcome of infection varies depending on the genetics of both the virus, and host. For instance, corneas of C57BL/6 mice infected with the RE strain of HSV-1 develop a transient epithelial lesion followed by the severe vascularization, leukocytic infiltration and edema that characterize HSK. In contrast, infection of the same mice strain with the same dose of the KOS strain of HSV-1 causes only an initial epithelial lesion with no clinically detectable inflammatory sequelae (Fig 1). This phenomenon appears to have a counterpart in humans, as many people periodically shed virus to the cornea asymptomatically [32] and even develop epithelial disease without progressing to HSK [7, 8, 33]. In fact, these relatively asymptomatic infections are sufficiently common to make one question whether they might provide some advantage to the host.

Here we examine the long-term changes to the microenvironment of the cornea resulting from KOS HSV-1 infections. We show that these infections, while not causing clinically detectable opacity and vascularization, do never-the-less result in significant long-term changes to the cornea. We showed that this includes a persistent infiltrate comprised predominantly of CD4$^+$ T cells, macrophages and elevated chemokines. Since these corneal changes are subclinical, they would not appear to compromise vision. We have observed and others have reported that subclinical HSV-1 corneal infections protect from subsequent infections with more virulent strains of HSV-1, and that protection is superior to immunity provided by i.p. or subcutaneous infection [34]. Moreover, protection is less effective or absent in MHC II knockout mice [35]. It is thus reasonable to conclude, that protection is due at least in part to residual CD4$^+$ T cells and macrophages in HSV-1 infected corneas with subclinical inflammation. Here, we posed two additional questions: regarding the subclinical inflammation in corneas following HSV-1 infection: 1) does it protect the cornea from unrelated pathogens expressing heterologous antigens; and 2) does it reduce the threshold for clinical inflammation induced by corneal trauma. We answer both questions in the affirmative.

We first employed a syngeneic corneal transplantation model to address the second question. We showed that syngeneic corneal grafts (that normally induce only very mild and transient corneal inflammation) induced more prolonged and robust inflammation when placed on KOS HSV-1 infected corneal bed with subclinical inflammation at 28-34 dpi. Our current data agree with our previous report in that opacity in syngeneic corneal grafts placed on

previously HSV-1 KOS infected corneas with subclinical inflammation did not reach a sustained opacity score of 12 (opacity of 3 in each quadrant of the graft) that would be considered to be a rejected or failed corneal graft [28]. However, the inflammation in syngeneic grafts placed on previously HSV-1 infected corneal beds was significant, and would be unacceptable in a human graft.

We further demonstrate that residual subclinical inflammation in previously HSV-1 infected corneas does provide a degree of innate resistance to the antigenicly unrelated pathogen PRV. The enhanced PRV clearance in corneas with subclinical inflammation was not dependent on pre-existing macrophages within the HSV-1 infected cornea, since clearance was not altered by a protocol that depleted resident macrophages but allowed macrophages to infiltrate after PRV infection (Fig 6). Thus, while infiltrating macrophages are likely involved in PRV clearance, tissue resident macrophages present in the previously HSV-1 infected corneas are not required. However, the enhanced innate resistance to PRV was abrogated by local depletion of $CD4^+$ T cells 3 days before PRV infection (Fig 7). This depletion strategy completely eliminated $CD4^+$ T cells from HSV-1 infected corneas 24 hr after PRV infection, suggesting that the $CD4^+$ T cells that persist in the cornea after KOS HSV-1 infections actively provide intrinsic resistance to subsequent PRV infection. While a possible explanation would be that $CD4^+$ T cells that infiltrate the cornea after HSV-1 infection recognize epitopes that are shared by PRV, however, we and others were unable to show such cross reactivity in $CD4^+$ T cells obtained from HSV-1 infected mice as previously shown [36-39]. While the relatively small number of $CD4^+$ T cells that persist in KOS HSV-1 infected corneas precluded a direct test of cross-reactivity, our data are inconsistent with antigenic cross-reactivity as the mechanism of enhanced PRV resistance in previously HSV-1 infected corneas. Thus, $CD4^+$ T cells that persist in corneas with subclinical inflammation following HSV-1 infection provide innate resistance to unrelated pathogens, likely through interaction with pre-existing or infiltrating macrophages.

We and others previously demonstrated that infections of BALB/c mice with HSV-1 KOS in the eye or the ear can cause loss of sensation proximal to the site of infection [9, 40, 41]. In the HSK mouse model, pathology is preceded by a complete loss of corneal sensory nerves and blink reflex, and is maintained by corneal stromal hyperinnervation by sympathetic nerves [9, 10]. Here, we show that KOS HSV-1 infections of C57BL/6 mice that do not lead to clinically detectable HSK do qualitatively change corneal innervation. KOS infected corneas contain both sympathetic and sensory nerves (Supplemental Fig 1). These changes were reproducibly seen in 14 KOS HSV-1 infected corneas. We concluded they were HSV-1 induced, as we never see sympathetic nerves in non-infected corneas [9, 10]. In other mouse models, it has been demonstrated that nerve damage alone is sufficient to increase inflammation in the cornea and rescind corneal immune privilege [42]. It remains to be determined whether these modest changes in corneal innervation and sensitivity following HSV-1 KOS infection of C57BL/6 mice result in, or contribute to, the subclinical inflammation that persists in the corneas remains to be determined.

While not the focus of this study, we did examine the PRV-induced corneal pathology following infection of HSV-1 KOS infected and non-HSV-1 infected corneas. Those not previously challenged with HSV-1 went on to develop opacity, significant loss of corneal

blink reflex and vascularization, while those that were previously HSV-1 KOS infected showed greatly diminished pathologies (Supplemental Fig 1E&F). Data ancillary to our focus on the corneal microenvironment indicated that mice previously infected with HSV-1 KOS also had smaller adaptive immune responses to PRV, as measured by the number of activated T cells in the draining lymph nodes and the total number proliferating T cells in the TG and draining lymph nodes at nine days post-PRV infection (Supplemental Fig 1G-K and data not shown).

Evidence that viral infections can confer innate protection against unrelated pathogens has been presented prior to our study. Chronic infections with a murine gamma herpes virus were found to induce a memory macrophage population that provided the mouse with an intrinsic resistance to unrelated pathogens. In that same study, it was tested whether HSV-1 could provide innate resistant novel infections. Unlike our study, the HSV-1 virus was introduced via i.p. injection and an unrelated pathogen through the airway. The authors were unable to show any non-specific protective effects of a previous HSV-1 infection against the unrelated pathogen [18]. However, the authors did speculate that local HSV-1 infections might provide a site-specific resistance to unrelated pathogens. Another study demonstrated that tissue resident memory (Trm) $CD8^+$ T cells remaining in a tissue following acute viral infection can provide intrinsic resistance to heterologous pathogens. However, in that study, the unrelated pathogen was administered along with cognate antigen recognized by the $CD8^+$ Trms [19]. To our knowledge, we are the first to demonstrate a local intrinsic protection mediated by $CD4^+$ T cells in response to an apparently subclinical viral infection. The clinical relevance of our findings is underscored by the fact that the protection was observed in the context of a common human infection. Unfortunately, this innate protection comes at a cost, as HSV-1 KOS infected corneas are also subject to increased inflammation when exposed to non-specific stimuli such as surgical trauma.

Supplementary Material

Refer to Web version on PubMed Central for supplementary material.

Acknowledgements

The authors are very grateful to Department of Ophthalmology administrative staff. Lori Young, Katie Kozak and Alice Lang were indispensable in communicating with vendors, regulatory agencies and other academic departments both in and outside the University of Pittsburgh. The authors would like to acknowledge Moira L. Geary for assistance in surgeries, animal handling and the evaluation of clinical disease. Stephen Harvey PhD assisted in the preparation of RNA, and worked closely with University of Pittsburgh Genomic Research Core. Finally, we would like to thank the University of Pittsburgh Genomic Research Core for assistance with the NanoString^R analysis.

Support: Public Health Service Grants EY05945, EY015291 & P30 EY008098, and unrestricted Grants from the Western Pennsylvania Eye Bank, Research to Prevent Blindness, Inc and The Eye &Ear Foundation of Pittsburgh

References

1. Mueller SN, Gebhardt T, Carbone FR, Heath WR. Memory T cell subsets, migration patterns, and tissue residence. Annu Rev Immunol. 2013; 31:137–61. [PubMed: 23215646]
2. Rowe AM, St Leger AJ, Jeon S, Dhaliwal DK, Knickelbein JE, Hendricks RL. Herpes keratitis. Prog Retin Eye Res. 2013; 32:88–101. [PubMed: 22944008]

3. Jones BR. The clinical features of viral keratitis and a concept of their pathogenesis. Proc R Soc Med. 1958; 51(11):917–24. [PubMed: 13614398]
4. Ouwendijk WJ, Geluk A, Smits SL, Getu S, Osterhaus AD, Verjans GM. Functional characterization of ocular-derived human alphaherpesvirus cross-reactive CD4 T cells. J Immunol. 2014; 192(8):3730–9. [PubMed: 24623134]
5. Maertzdorf J, Verjans GM, Remeijer L, van der Kooi A, Osterhaus AD. Restricted T cell receptor beta-chain variable region protein use by cornea-derived CD4+ and CD8+ herpes simplex virus-specific T cells in patients with herpetic stromal keratitis. J Infect Dis. 2003; 187(4):550–8. [PubMed: 12599071]
6. Darougar S, Wishart MS, Viswalingam ND. Epidemiological and clinical features of primary herpes simplex virus ocular infection. Br J Ophthalmol. 1985; 69(1):2–6. [PubMed: 3965025]
7. Liesegang TJ. Epidemiology of ocular herpes simplex. Natural history in Rochester, Minn, 1950 through 1982. Arch Ophthalmol. 1989; 107(8):1160–5. [PubMed: 2757546]
8. Labetoulle M, Auquier P, Conrad H, Crochard A, Daniloski M, Bouee S, El Hasnaoui A, Colin J. Incidence of herpes simplex virus keratitis in France. Ophthalmology. 2005; 112(5):888–95. [PubMed: 15878072]
9. Yun H, Rowe AM, Lathrop KL, Harvey SA, Hendricks RL. Reversible nerve damage and corneal pathology in murine herpes simplex stromal keratitis. J Virol. 2014; 88(14):7870–80. [PubMed: 24789786]
10. Yun H, Lathrop KL, Hendricks RL. A Central Role for Sympathetic Nerves in Herpes Stromal Keratitis in Mice. Invest Ophthalmol Vis Sci. 2016; 57(4):1749–56. [PubMed: 27070108]
11. Gimenez F, Suryawanshi A, Rouse BT. Pathogenesis of herpes stromal keratitis--a focus on corneal neovascularization. Prog Retin Eye Res. 2013; 33:1–9. [PubMed: 22892644]
12. Chucair-Elliott AJ, Zheng M, Carr DJ. Degeneration and regeneration of corneal nerves in response to HSV-1 infection. Invest Ophthalmol Vis Sci. 2015; 56(2):1097–107. [PubMed: 25587055]
13. Masopust D, Vezys V, Marzo AL, Lefrancois L. Preferential localization of effector memory cells in nonlymphoid tissue. Science. 2001; 291(5512):2413–7. [PubMed: 11264538]
14. Gebhardt T, Wakim LM, Eidsmo L, Reading PC, Heath WR, Carbone FR. Memory T cells in nonlymphoid tissue that provide enhanced local immunity during infection with herpes simplex virus. Nat Immunol. 2009; 10(5):524–30. [PubMed: 19305395]
15. Wertheim JO, Smith MD, Smith DM, Scheffler K, Kosakovsky Pond SL. Evolutionary origins of human herpes simplex viruses 1 and 2. Mol Biol Evol. 2014; 31(9):2356–64. [PubMed: 24916030]
16. Shen JH, Huang KY, Chao-Yu C, Chen CJ, Lin TY, Huang YC. Seroprevalence of Herpes Simplex Virus Type 1 and 2 in Taiwan and Risk Factor Analysis, 2007. PLoS One. 2015; 10(8):e0134178. [PubMed: 26252011]
17. Kasubi MJ, Nilsen A, Marsden HS, Bergstrom T, Langeland N, Haarr L. Prevalence of antibodies against herpes simplex virus types 1 and 2 in children and young people in an urban region in Tanzania. J Clin Microbiol. 2006; 44(8):2801–7. [PubMed: 16891495]
18. Barton ES, White DW, Cathelyn JS, Brett-McClellan KA, Engle M, Diamond MS, Miller VL, Virgin H.W.t. Herpesvirus latency confers symbiotic protection from bacterial infection. Nature. 2007; 447(7142):326–9. [PubMed: 17507983]
19. Schenkel JM, Fraser KA, Beura LK, Pauken KE, Vezys V, Masopust D. T cell memory. Resident memory CD8 T cells trigger protective innate and adaptive immune responses. Science. 2014; 346(6205):98–101. [PubMed: 25170049]
20. Posavad CM, Zhao L, Mueller DE, Stevens CE, Huang ML, Wald A, Corey L. Persistence of mucosal T-cell responses to herpes simplex virus type 2 in the female genital tract. Mucosal Immunol. 2015; 8(1):115–26. [PubMed: 24917455]
21. Mackay LK, Stock AT, Ma JZ, Jones CM, Kent SJ, Mueller SN, Heath WR, Carbone FR, Gebhardt T. Long-lived epithelial immunity by tissue-resident memory T (TRM) cells in the absence of persisting local antigen presentation. Proc Natl Acad Sci U S A. 2012; 109(18):7037–42. [PubMed: 22509047]

22. Chen SH, Pearson A, Coen DM, Chen SH. Failure of thymidine kinase-negative herpes simplex virus to reactivate from latency following efficient establishment. J Virol. 2004; 78(1):520–3. [PubMed: 14671133]

23. Lausch RN, Oakes JE, Metcalf JF, Scimeca JM, Smith LA, Robertson SM. Quantitation of purified monoclonal antibody needed to prevent HSV-1 induced stromal keratitis in mice. Curr Eye Res. 1989; 8(5):499–506. [PubMed: 2736955]

24. Bowen CD, Renner DW, Shreve JT, Tafuri Y, Payne KM, Dix RD, Kinchington PR, Gatherer D, Szpara ML. Viral forensic genomics reveals the relatedness of classic herpes simplex virus strains KOS, KOS63, and KOS79. Virology. 2016; 492:179–86. [PubMed: 26950505]

25. Du T, Zhou G, Roizman B. HSV-1 gene expression from reactivated ganglia is disordered and concurrent with suppression of latency-associated transcript and miRNAs. Proc Natl Acad Sci U S A. 2011; 108(46):18820–4. [PubMed: 22065742]

26. Szabo SJ, Sullivan BM, Stemmann C, Satoskar AR, Sleckman BP, Glimcher LH. Distinct effects of T-bet in TH1 lineage commitment and IFN-gamma production in CD4 and CD8 T cells. Science. 2002; 295(5553):338–42. [PubMed: 11786644]

27. Plskova J, Kuffova L, Holan V, Filipec M, Forrester JV. Evaluation of corneal graft rejection in a mouse model. Br J Ophthalmol. 2002; 86(1):108–13. [PubMed: 11801514]

28. Kuffova L, Knickelbein JE, Yu T, Medina C, Amescua G, Rowe AM, Hendricks RL, Forrester JV. High-Risk Corneal Graft Rejection in the Setting of Previous Corneal Herpes Simplex Virus (HSV)-1 Infection. Invest Ophthalmol Vis Sci. 2016; 57(4):1578–87. [PubMed: 27050878]

29. Medina CA, Rowe AM, Yun H, Knickelbein JE, Lathrop KL, Hendricks RL. Azithromycin treatment increases survival of high-risk corneal allotransplants. Cornea. 2013; 32(5):658–66. [PubMed: 23407315]

30. Lepisto AJ, Frank GM, Xu M, Stuart PM, Hendricks RL. CD8 T cells mediate transient herpes stromal keratitis in CD4-deficient mice. Invest Ophthalmol Vis Sci. 2006; 47(8):3400–9. [PubMed: 16877409]

31. Hazlett LD, Hendricks RL. Reviews for immune privilege in the year 2010: immune privilege and infection. Ocul Immunol Inflamm. 2010; 18(4):237–43. [PubMed: 20662654]

32. Kaufman HE, Azcuy AM, Varnell ED, Sloop GD, Thompson HW, Hill JM. HSV-1 DNA in tears and saliva of normal adults. Invest Ophthalmol Vis Sci. 2005; 46(1):241–7. [PubMed: 15623779]

33. Liesegang TJ. Herpes simplex virus epidemiology and ocular importance. Cornea. 2001; 20(1):1–13. [PubMed: 11188989]

34. Nesburn AB, Slanina S, Burke RL, Ghiasi H, Bahri S, Wechsler SL. Local periocular vaccination protects against eye disease more effectively than systemic vaccination following primary ocular herpes simplex virus infection in rabbits. J Virol. 1998; 72(10):7715–21. [PubMed: 9733807]

35. Ghiasi H, Perng GC, Hofman FM, Cai S, Nesburn AB, Wechsler SL. Specific and nonspecific immune stimulation of MHC-II-deficient mice results in chronic HSV-1 infection of the trigeminal ganglia following ocular challenge. Virology. 1999; 258(2):208–16. [PubMed: 10366558]

36. Enquist LW, Dubin J, Whealy ME, Card JP. Complementation analysis of pseudorabies virus gE and gI mutants in retinal ganglion cell neurotropism. J Virol. 1994; 68(8):5275–9. [PubMed: 8035525]

37. Enquist LW, Miselis RR, Card JP. Specific infection of rat neuronal circuits by pseudorabies virus. Gene Ther. 1994; 1(Suppl 1):S10. [PubMed: 8542382]

38. Koyuncu OO, Perlman DH, Enquist LW. Efficient retrograde transport of pseudorabies virus within neurons requires local protein synthesis in axons. Cell Host Microbe. 2013; 13(1):54–66. [PubMed: 23332155]

39. Brittle EE, Reynolds AE, Enquist LW. Two modes of pseudorabies virus neuroinvasion and lethality in mice. J Virol. 2004; 78(23):12951–63. [PubMed: 15542647]

40. Takahashi H, Hato N, Honda N, Kisaki H, Wakisaka H, Matsumoto S, Gyo K. Effects of acyclovir on facial nerve paralysis induced by herpes simplex virus type 1 in mice. Auris Nasus Larynx. 2003; 30(1):1–5. [PubMed: 12589842]

41. Murakami S, Hato N, Mizobuchi M, Doi T, Yanagihara N. Role of herpes simplex virus infection in the pathogenesis of facial paralysis in mice. Ann Otol Rhinol Laryngol. 1996; 105(1):49–53. [PubMed: 8546424]

42. Paunicka KJ, Mellon J, Robertson D, Petroll M, Brown JR, Niederkorn JY. Severing corneal nerves in one eye induces sympathetic loss of immune privilege and promotes rejection of future corneal allografts placed in either eye. Am J Transplant. 2015; 15(6):1490–501. [PubMed: 25872977]

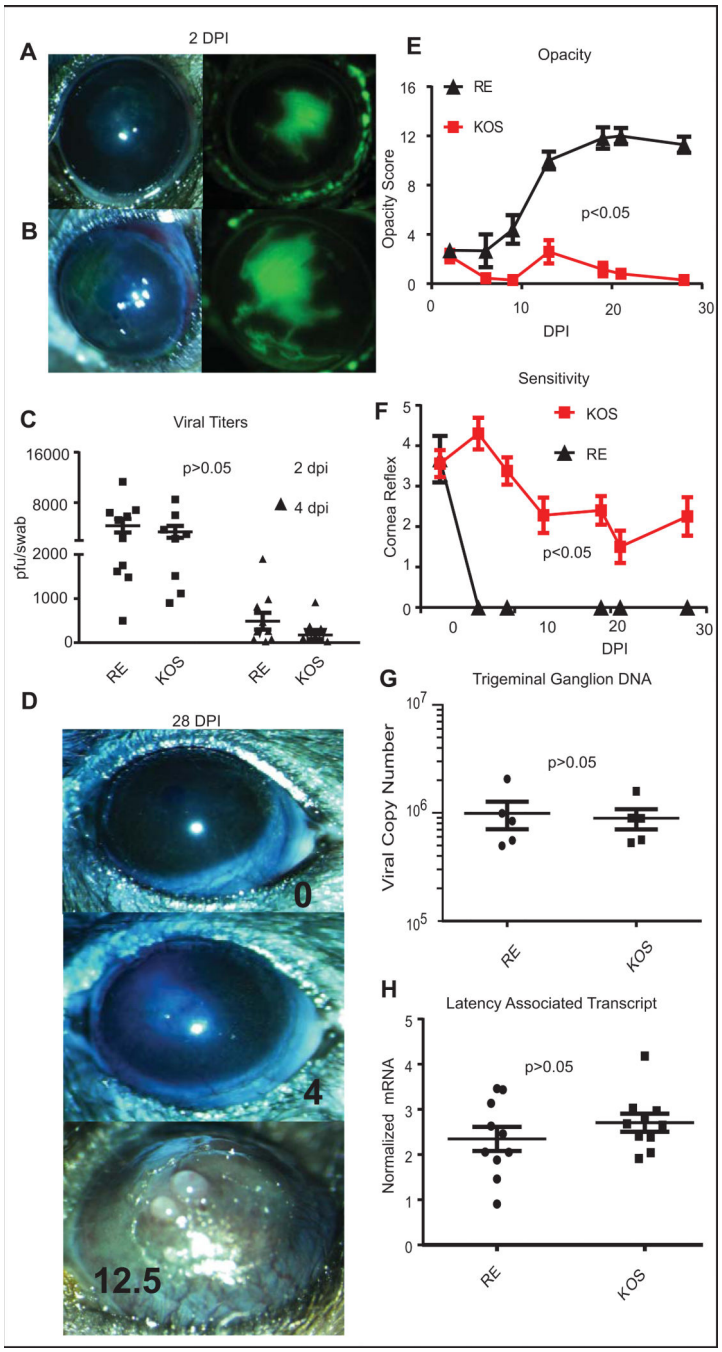

Figure 1. Corneal pathology induced by RE and KOS HSV-1 infections

Photomicrographs of C57BL/6 corneas were obtained 2 days after infection with $1x10^5$ pfu per eye of HSV-1 RE (**A**) or HSV-1 KOS (**B**) and lesions were visualized with fluorescein sodium (green). Viral titers were assessed in eye swabs obtained at 2 and 4 dpi using a standard plaque assay **(C)**, and the significance of differences in mean titers of the two viruses was assessed by two-way ANOVA. Photomicrographs obtained at 28 dpi **(D)** show the absence of overt pathology typically observed in KOS infected mice **(top panel)**. A small fraction of KOS infected mice did show mild opacity **(middle panel)** and these mice

were excluded from subsequent experiments described in other figures. RE HSV-1-infected corneas exhibit typical severe HSK **(bottom panel)**. Opacity scores (12 point scale) are listed. Corneal opacity was tracked over time **(E)** with n=20 HSV-1 KOS infected and n=14 HSV-1 RE infected corneas from pooled experiments. Mice were monitored for corneal sensitivity by touching the four quadrants of the peripheral cornea and the central cornea and recording the number of areas of each cornea that retained blink reflex. A score of 5 indicates complete responsiveness in all areas of the cornea test and score of 0 indicates a cornea lacking reflex to palpation of any area of the cornea. **(F)** n=25 HSV-1 KOS infected, n=10 HSV-1 RE infected from pooled experiments. RE HSV-1 infected corneas completely lost sensation, while KOS infected corneas all retained at least partial sensation. For both opacity **(E)** and sensitivity **(F)** the area under the curve was calculated for each cornea and p values for group differences determined by a Student's T-test for each experiment. Trigeminal ganglia (TG) were obtained from KOS and RE HSV-1 infected mice at 28-34 dpi, DNA or RNA was extracted, and the viral genome copy number per TG quantified by qPCR **(G)** or levels of Latency Associated Transcript (LAT) mRNA were quantified by qRT-PCR normalized to the expression of histone H1 host gene. Viral genome copies and LAT expression were compared via student's T-test (data are representative of 1 of 4 experiments for genome comparison and of 1 of 3 experiments for LAT comparison).

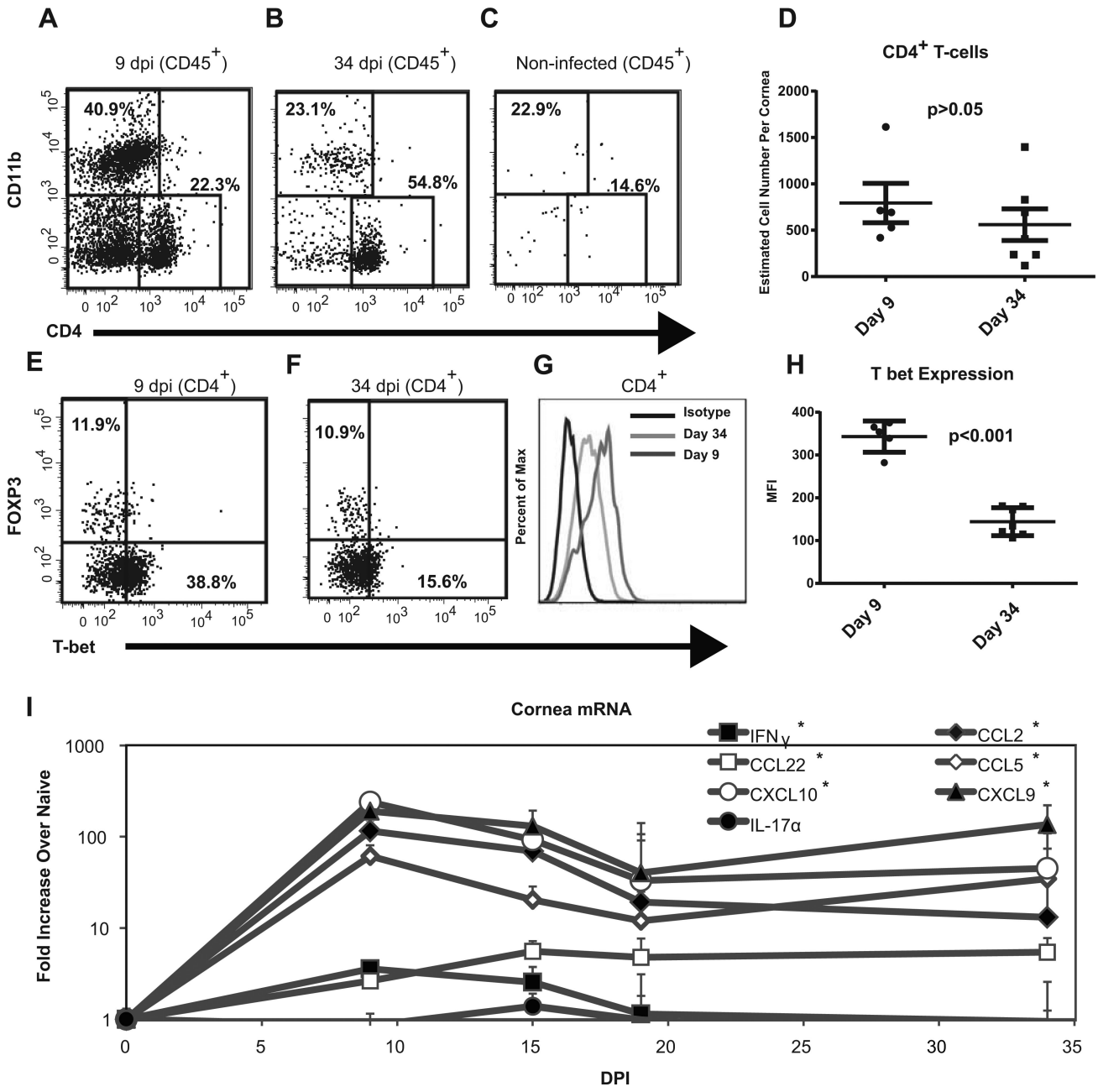

Figure 2. Persistent subclinical inflammation in KOS HSV-1 infected corneas

The corneas of female C57BL/6 mice were infected with 1×10^5 pfu of HSV-1 KOS, excised at 9 dpi **(A, E, D, G, H)** or 34 dpi **(B, F, D, G, H),** stained for surface CD45, CD4, CD11b, and TCRβ and for intracellular T-bet and Foxp3, and were analyzed by flow cytometry. Non-infected corneas were included for comparison. Representative flow plots gated on $CD45^+$ cells show the frequency of $CD4^+$ and $CD11b^+$ cells **(A-C)**. TCRβ was expressed on all $CD4^+$ but no $CD11b^+$ cells (not shown). The absolute number of $CD45^+CD4^+$ $TCR\beta^+$ cells/cornea is shown with the mean and SEM represented by horizontal and vertical lines, respectively **(D)**. The $CD45^+CD4^+$ $TCR\beta^+$ were analyzed for Foxp3 and T-bet (**E-H**). A histogram **(G)** and graph of mean fluorescence intensity (MFI) **(H)** for T-bet staining in

$CD4^+$ T cells from pools of corneas is shown (T-bet and FOXP3 data is representative of 1 of 2 experiments). The values were compared via student's T-test. Total RNA was extracted from HSV-1 KOS infected corneas obtained at various times after infection and analyzed for cytokine and chemokine mRNA using nanostring technology **(I)** n=3-5 mice per time point. Transcript levels are recorded as a fold increase over that observed in non-infected (naïve) corneas. Relative gene expression over time was compared using a Kruskal-Wallis test, (*) indicates a $p < 0.05$.

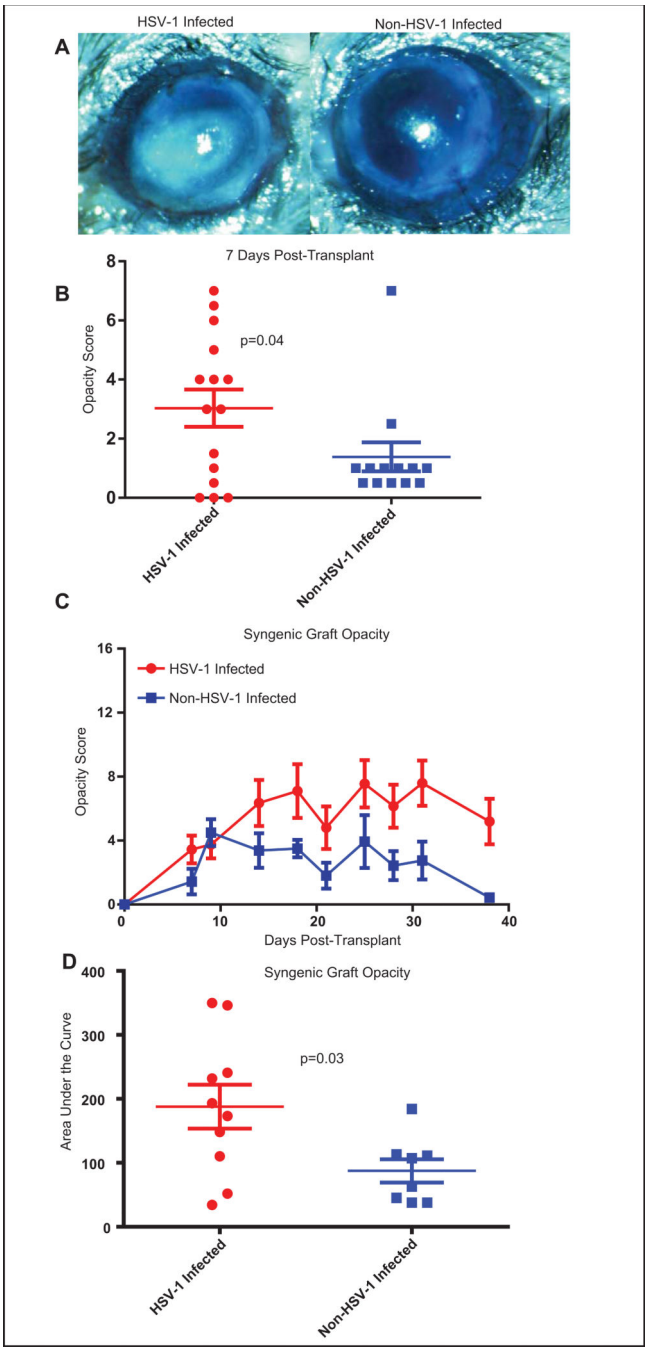

Figure 3. Previously HSV-1 infected corneas with subclinical inflammation show a more robust response to surgical insult

Corneas of female C57BL/6 mice were infected with 1×10^5 pfu of KOS HSV-1. At 34 dpi, previously infected corneas with subclinical inflammation or non-infected corneas were recipients of non-infected syngeneic corneal grafts. All transplanted eyes received a temporary tarsorrhaphy directly following transplant. Seven days after transplant the tarsorrhaphy was removed and the eyes were examined. Corneal grafts placed on previously infected beds exhibited greater opacity **(A, left panel)** compared to those placed on non-infected beds **(A, right panel)** seven days after transplant. Graft opacity was scored on a 16

point scale at 7 day post-transplant and group means compared via Kolmogorov-Smirnov test **(B).** Data are representative of 4 independent experiments. Graft opacity was evaluated over a five week period post-transplant **(C)**, and the area under the curve (AUC) for individual mice **(D)** was compared via students T-test. Data are from a single experiment representative of two repeats.

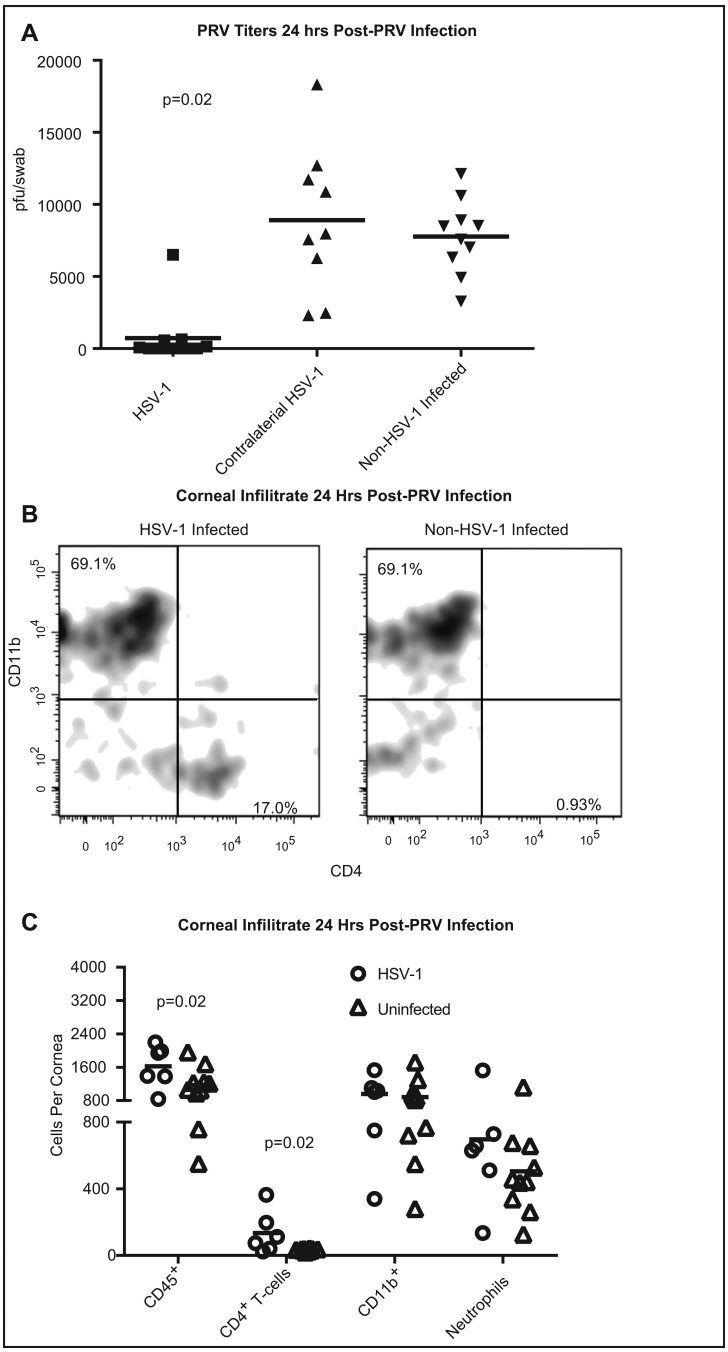

Figure 4. Previously HSV-1 infected corneas with subclinical inflammation rapidly resolve PRV infections

Corneas of female C57BL/6 mice were infected with 1×10^5 pfu of KOS HSV-1. At 34 dpi, previously infected corneas with subclinical inflammation, the non-infected contralateral cornea, or corneas of non-infected mice were challenged with 1×10^5 pfu of PRV. At 24 hrs **(A)** and 96 hrs (not shown) post-PRV challenge the eyes were swabbed and PRV pfu per swab was determined using a plaque assay. Group means were compared by a Kruskal-Wallis one-way ANOVA ($p<0.001$) and individual groups compared by a Dunn's post-test. Previously infected corneas had significantly ($p= 0.02$) lower titers than non-infected

contralateral corneas or corneas of non-infected mice Single cell suspensions of individual corneas obtained 24 hrs after PRV challenge were: stained for CD45, CD4 and CD11b and flow plots gated on CD45 show the frequency of each population **(B)**; or corneal cells were stained for CD45, CD4, CD11b, Gr-1, and Ly6C and absolute numbers of $CD45^{+}$ leukocytes; $CD4^{+}$, $CD11b^{-}$ T cells; $CD11b^{+}$, $Ly6C^{High}$, $Gr\text{-}1^{Int}$ macrophages, and $CD11b^{+}$, $Gr\text{-}1^{High}$, $Ly\text{-}6C^{low}$ neutrophils were quantified in each cornea **(C)**. The number of cells in each population was compared via T-test and p values are shown for groups with significant differences. The data are from a single experiment that was repeated six times.

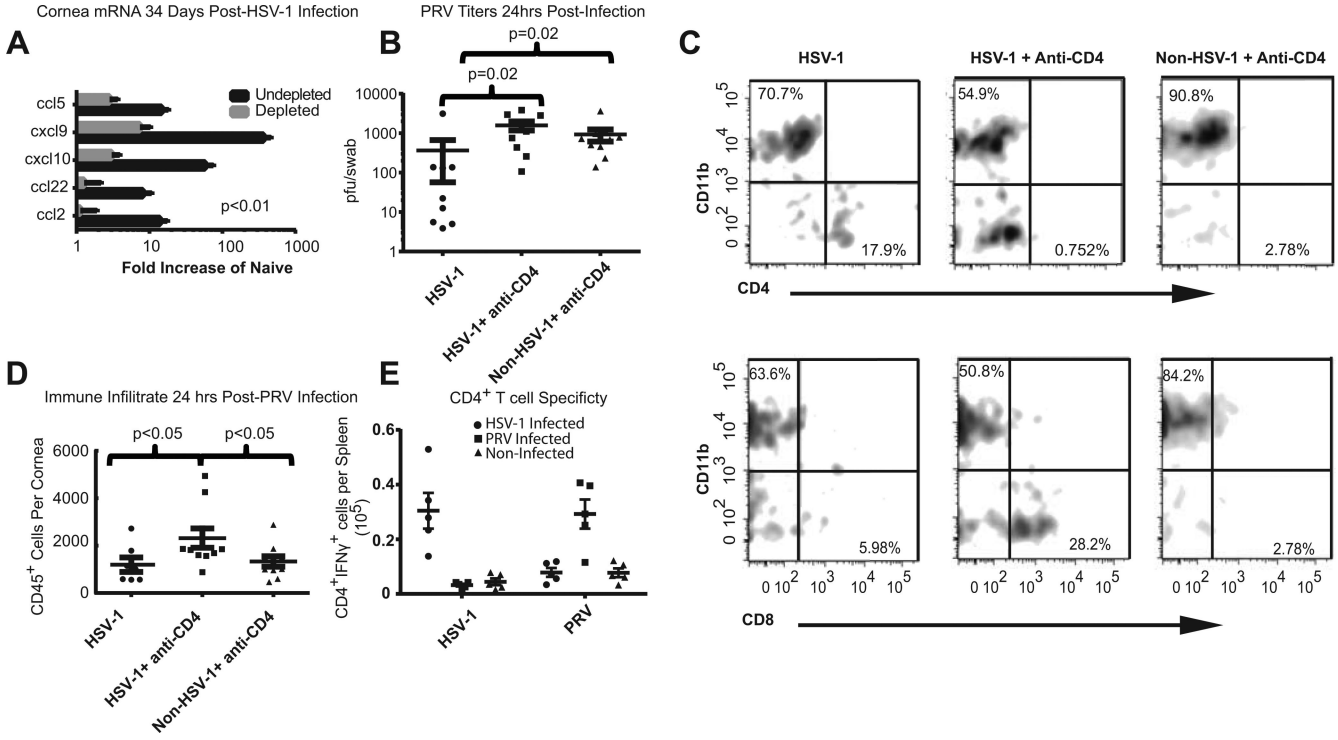

Figure 5. A CD4$^+$ T cell response is required for HSV-1 mediated protection from PRV

C57BL/6 mice were depleted of CD4$^+$ T cells by weekly i.p. injections with anti-CD4 antibody beginning 2 days prior to HSV-1 KOS infection or mock infection and continuing at weekly intervals until 34 dpi. HSV-1 infected corneas of mice that were not CD4-depleted or CD4-depleted corneas that were not HSV-1 infected served as controls. Corneas were excised at 34 dpi, RNA extracted, and chemokine transcripts were quantified using a Nanostring probe set **(A)**. All group differences were significant ($p<0.001$) when assessed using a one-way ANOVA (n=5 for CD4-depleted, 4 for non-depleted). The experiment was repeated with similar results. The HSV-1 infected corneas of CD4$^+$ T cell-depleted and non-depleted mice or corneas that were CD4-depleted but not HSV-1 infected were challenged with 1×10^5 pfu of PRV 28-34 days after HSV-1 infection. Eye swabs were obtained 24 hrs later and PRV pfu determined in a plaque assay **(B)**. The groups were compared by a Kruskal-Wallis one-way ANOVA and Dunn's multiple comparison test and data is representative of 1 of 2 experiments. Single cell suspensions of individual corneas obtained 24 hrs after PRV infection were stained for CD45, CD11b, CD4, and CD8 and analyzed by flow cytometry. Representative flow plots show a CD4$^+$ T cell population in HSV-1 infected corneas that were mock CD4-depleted that was not present in HSV-1 infected corneas that were CD4-depleted or in corneas that were not previously HSV-1 infected **(C, upper panels).** CD8$^+$ T cells were prominently present in CD4$^+$ T cell-depleted corneas after PRV infection, but were largely absent from corneas of CD4$^+$ T cell-replete mice that were HSV-1 infected or non-infected **(C, lower panels).** The overall CD45 leukocytic infiltrate is recorded as absolute number of cells/cornea **(D),** and group means compared by a one-way ANOVA with Tukey's post-tests. CD4$^+$ splenocytes were obtained from mice 9 days after corneal infection with 1×10^5 pfu of HSV-1 (filled circles) or PRV (filled squares) and from Non-Infected mice (filled triangles). The CD4$^+$ T cells were co-cultured for 5 hours in the

presence of Brefeldin-A with splenocytes from non-infected C57BL/6 mice that were T cell depleted and infected *in vitro* with HSV-1 or PRV. Cells were then stained for surface CD4 and intracellular IFN-γ and analyzed by flow cytometry **(E)**. Values were compared within groups stimulated with the same APCs via a one-way ANOVA and between groups using a two-way ANOVA. There was no significant cross reactivity. Data is representative of one of two experiments.

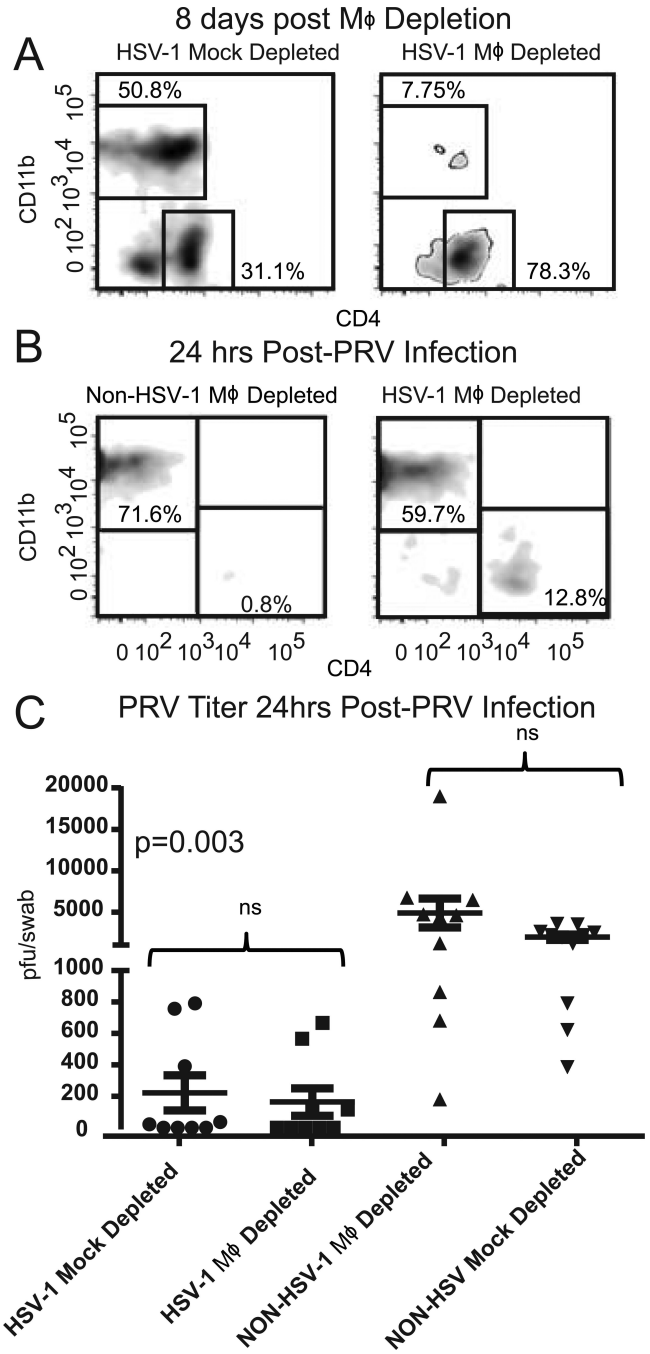

Figure 6. Cornea resident macrophages are not required for HSV-1 mediated resistance to PRV

C57BL/6 mice that received HSV-1 corneal infections 28-34 days previously or non-infected controls received a single subconjunctival injection of clodronate liposomes and anti-Ly6C antibody (MΦ depleted) or an injection with PBS liposomes (Mock depleted). At 8 days post-injection corneal single cell suspensions were stained for CD45, CD11b, and CD4 and analyzed by flow cytometry gated on CD45 to demonstrate the efficacy of MΦ depletion from the cornea prior to PRV infection **(A)**. The MΦ-deplete and mock-depleted corneas were then infected with 1×10^5 pfu of PRV, and single cell suspensions of corneal cells were

stained for CD45, CD4 and CD11b and analyzed by flow cytometry gated on CD45 **(B)**. Corneas were swabbed at 24 hrs after corneal PRV infection and PRV titers were assessed by a viral plaque assay and recorded as PRV pfu/swab (C). The significance of group differences in PRV titers was assessed by a Kurskal-Wallis test followed by Dunn's multiple comparison test. Data is representative of 1 of 3 experiments.

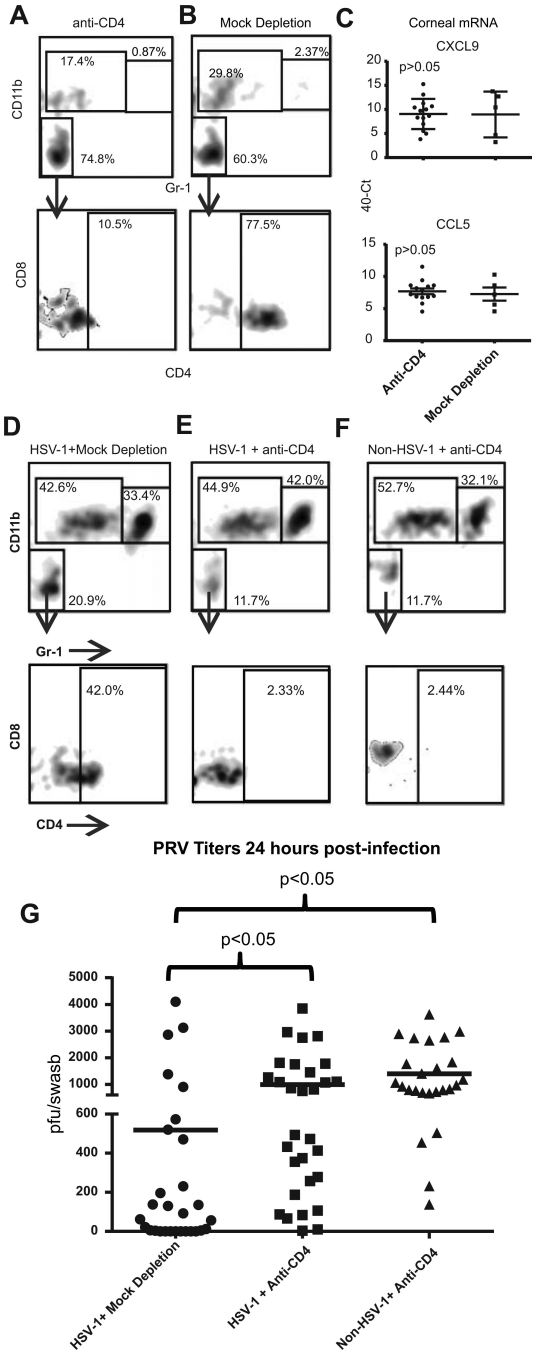

Figure 7. Corneal CD4$^+$ T cells mediate HSV-1-induced resistance to PRV infection

C57BL/6 mice that received HSV-1 corneal infections 28-34 days previously or non-infected controls received local (subconjunctival) injections of anti-CD4 antibody (CD4-depleted) or control antibody (Mock-depleted). Corneas were excised 3days later and single cell suspensions were stained for CD45, CD4, CD8, CD11b, and Gr-1 and analyzed by flow cytometry **(A & B)** initially gating on CD45 cells and analyzing for CD11b and Gr-1 (top row) and then gating on the double-negative population and analyzing for CD8 and CD4 (bottom row). The frequency of cells within each area of the flow plot is shown.

Alternatively, total RNA was extracted from the HSV-1 infected and CD4-depl or Mock-depleted corneas and CXCL9 and CCL5 chemokine transcripts were quantified by qRT-PCR **(C).** Data is representative of 1 of 3 experiments in the case of CXCL9 and 1 of 2 experiments regarding CCL5. The HSV-1 infected or mock infected corneas that were CD4-depleted or Mock-depleted were then infected with 1×10^5 pfu of PRV and 24 hrs later the corneas were excised and single cell suspensions of corneal cells were stained and analyzed by flow cytometry as described above **(D-F)**. Corneal swabs were obtained 24 hrs after PRV infection, infectious PRV was quantified using a viral plaque assay, and results reported as pfu/swab **(G)**. The significance of group differences PRV pfu was assessed by a Kurskal-Wallis test followed by Dunn's multiple comparison test. Data is pooled from three independent experiments.

Table I

Common Gene Names and the NCBI Reference Sequences for the mRNA molecules assayed by Nanostring[R].

	NanoString Target Sequences	
	Common Gene Name	**Sequence ID**
Genes Assayed By Nanostring	IFN gamma	NM_008337.1
	IL-10	NM_010548.1
	IL-10R	NM_008348.2
	Ccl2	NM_011333.3
	Ccl22	NM_009137.2
	Ccl5	NM_013653.1
	Cxcl10	NM_021274.1
	Cxcl9	NM_008599.2
	IL-17alpha	NM_010552.3
	GAPDH	NM_001001303.1
House Keeping Genes	Laminin B-1	NM_008482.2
	Ribosomal Protein 5	NM_016980.2
	ubiquitin C	NM_019639.4